Supplementary Information

1) Active site model and computational enzyme design

Distances, angles and dihedrals of the corresponding active sites were measured for all interacting inhibitor-residue atom pairs as shown in Table S1: Zn to $O\varepsilon^1$ or $O\varepsilon^2$ atoms for Glu_{cat} and Zn to $N\varepsilon^2$ atoms for His_{1-3}; periodicity of 360° was set for all geometrical parameters except for χ_{AB} in His_{1-3} where it was set to 11.25°, corresponding to discrete rotation of the imidazole ring around the Cβ-Cγ bond. Interactions were modelled as pseudocovalent for His_{1-3}-Zn and as non-bonded for Glu_{cat}-Zn, with higher *k* values for distances than for angles and dihedrals to penalize designs with distorted coordination geometries. Two parameter sets were used to sample the *x0±xtol* value range at regular intervals: the first with *n*=1 to sample 2*n*+1=5 discrete values for all 6 geometrical parameters; the second with the "rule-of-thumb" *n=xtol/0.1* for d_{AB} and *n=xtol/5* for remaining geometrical parameters (*n<4,* maximum 9 discrete values). The first set was used to screen and design NMR structures; the second set was used to screen and design X-ray structures since it allows increased conformational sampling of side chain orientations. The 2010 Dunbrack rotamer library was used, with $\chi'_{1,2}\pm 2\sigma$ side chain sampling for His_{1-3}. The model substrate diAla was based on atomic coordinates of the high-resolution structure of astacin with bound inhibitor molecule (PDB ID: 1QJI).[1] The Inhibitor was trimmed and the phosphate atom replaced by a carbon atom. This allowed for reconstruction of alanine side chains in extended conformation. Conformers were generated with the Open Babel software [2]: 6 rotatable bonds identified, 7776 conformers tested and final 306 conformers produced, including the original extended conformer. The corresponding files and options used as input for Rosetta are described in Table S2. The resulting Rosetta *cst* file of the model active site is shown in Table S3.

The options used for both the *matcher and enzyme design* executables are given along active site definition in Table S3. The complete list of obtained designs is shown in Table S4. The final step of design did not evaluate repacking in the absence of diAla, as reference for REU calculation, sincezinc was modelled as part of the substrate (charge repulsion in the absence of zinc render the pre-organization of His_{1-3} unfavourable). The parameters used to build the correlation matrix were: *total_score* ($Score_{total}$), *fa_rep* (repulsive LJ), *hbond_sc* (H-bond energy), *all_cst* (constraint, k), *tot_pstat_pm* (Packing), *tot_nlsurfaceE_pm* (surface energy), *SR_1_total_score* (Glu_{cat}), *SR_2_total_score* (His_1), *SR_3_total_score* (His_2), *SR_4_total_score* (His_3), *SR_5_total_score* ($diAla_{score}$), *SR_5_fa_rep* (diAla repulsive LJ), *SR_5_hbond_sc* (diAla H-bond energy), *SR_5_all_cst* (diAla constraint, k), *SR_5_interf_E_1_2* (diAla interface energy), and *SR_5_dsasa_1_2* (diAla solvent accessible surface area, SASA). Sequence length (L) was included as an additional parameter to account for the system size variability. This set does not contain scaffold-specific parameters, such as pose metric calculators. For enhanced discrimination of results, the parameters related with constraint penalty *k*, *all_cst* and *SR5_all_cst*, were represented in *k* logarithm scale. Results of PCA analysis are given in Figure S1.

2) List of reagents and equipment

Synthesis of peptides was done in an Initiator+ Alstra Automated Microwave Peptide Synthesizer (Biotage) or in a Liberty Microwave-Assisted Automated Peptide Synthesizer (CEM GmbH) using the supplier's protocols and optimized accordingly to the methods developed in our laboratory. Fmoc-amino acids were purchased from CEM, Novabiochem (now Merk GmBH) and Iris Biotech GmbH. Rink Amide 4-methylbenzhydrylamine (100-200 mesh, loading 0.59 mmol/g or 100-200 mesh, loading 0.36mmol/g) resin and 2-(1H-Benzotriazole-1-yl)-1,1,3,3-tetramethyluronium hexafluorophosphate were obtained from Novabiochem. Trifluoroacetic acid, anisole, thioanisole, 1,2-ethanedithiol, triisopropylsilane, 1-hydroxybenzotriazole and piperidine were acquired from Merck. Acetonitrile, dimethylformamide, diethyl ether, dichloromethane, N-methyl-2-pyrrolidone, N,N-diisopropylethylamine, acetic anhydride and triethylamine were obtained from different commercial suppliers. All reagents used were the highest grade available. DiAla was purchased from POP-UP (Peptide Synthesis Facility at University of Porto, Portugal) with a purity of 92% and used without further purification. Preparative HPLC was made using linear gradient methods with mobile phase of solvent A (H_2O/TFA 99.9:0.1 v/v) and solvent B (ACN/H_2O/TFA 90:9.9:0.1 v/v), using a C18 Phenomenex Jupiter 250 mm x 21.2 mm, 15 µm 300 Å column. Analytical HPLC was made with the same methods adapted accordingly in either a Phenomenex C12 Jupiter Proteo, 250 mm x 4.6 mm, 4 µm, 300 Å or C18 Phenomenex Jupiter 250 mm x 4.6 mm, 15 µm, 300 Å and Discovery HS 250 mm x 4.6 mm, 5 µm. CD spectroscopy was performed in a Jasco J-815 CD spectropolarimeter (Integration time 1 or 2 seg, bandwidth 1 or 2 nm, 8 accumulations, scan speed 100 nm/min) with external temperature controller Jasco CDF-426S/15 or Applied Photophysics Chirascan™ qCD spectrometer (Integration time 3 s, bandwidth 1 nm, 3 accumulations, scan speed 20 nm/min). UV-Vis spectroscopy was performed in a Cary 100 Bio spectrophotometer with a Peltier temperature controller or in 96-well plates at room temperature in a Tecan Infinite F200 microplate reader. NMR spectroscopy was performed in a Bruker Avance II+ 800 MHz or Bruker Avance II+ 500 MHz. Assays done at different pH values used compositions shown in Table S5.

3) Zinc binding, thermal stability and hydrolytic activity

For CD spectroscopy, the signal (θ_{obs}) was converted from ellipticity to mean residual weight ($[\theta]_{MRW}$) in units of deg.dmol.cm^2 by the equation 1:

$$[\theta]_{MRW} = \frac{\theta_{obs}}{10lcm} \qquad (1)$$

where *l* is the path-length of cell, 10 is the conversion factor from mol to dmol, *c* is the molar concentration of peptide (mol/L) and *m* is the number of peptide bonds in case of Sp1f2/RD01 (m= 30) and HP35/RD02 (m= 34).

For esterase activity determination using 4-nitrophenyl acetate, the rates of product formation k_{obs} were calculated by equation 2:

$$k_{obs}(M.s^{-1}) = \frac{A_{400}}{l\varepsilon} \times \frac{1}{s} = \frac{[4\text{-}nP]}{s} \qquad (2)$$

where A_{400} was converted to [4-nP] using ε_{400} according to Table S5. Linearity considered when $R^2 > 0.99$ over recorded time. The ε_{400} values were determined under the same experimental conditions for

each pH (including 5% ACN) by measuring A_{400} values of product 4-nitrophenol. Rates of product formation obtained for control assays were subtracted in the corresponding catalyst assays (free peptide and zinc complex). The [Zn]/[RD] used for each pH was chosen according to Figure S4. The first order rate constant V_{cat} was calculated accordingly for assays with different concentrations of catalyst by equation 3:

$$V_{cat}(s^{-1}) = (k_{obs,catalyst} - k_{obs,background}) \times \frac{1}{[catalyst]} \qquad (3)$$

Second-order rate constant k_2 was calculated according to equation 4:

$$k_2\ (M^{-1}s^{-1}) = \frac{V_{cat}}{[4-nPA]} \qquad (4)$$

Single amino acid p-nitroanilides (X-pNA, where X= Ala, Gly, Glu, Arg, Met, Leu) were purchased from Sigma-Aldrich and 100 mmol/L stock solutions were prepared in corresponding solvents (acetone, acetonitrile or water). The formation of the product p-nitroaniline (pNA) was monitored by following A_{405} increase under the experimental conditions described for esterase assays over a period of at least 2 days. The extinction coefficient of product aniline, ε_{405}=5329 $M^{-1}cm^{-1}$ from a nitroaniline solution. The ab112146 MMP Activity Assay Kit (fluorometric – green) was purchased from Abcam and assays were performed according to the provided protocol. Fluorescence signal was monitored in microplate format at room temperature (V_T= 100 µL) with an Ex/Em = 490/525 nm for variable time intervals up to a total duration of 2 days. A 1 mM diAla stock solution was prepared in D_2O 50mM NaCl (molecular weight 201.11 g/mol, 0.2 mg/mL) and its pH adjusted to 7.47 with additions of concentrated NaOH and HCl solutions. Assays were done by direct addition of both 25 µM peptide and 75 µM $ZnCl_2$ to diAla 1 mM solutions (V_T= 600 µL). ^{1}H NMR spectra were recorded immediately after the addition of peptide and metal to 1 mM diAla solution and followed at variable time intervals up to a total duration of at least 2 days.

4) Molecular Dynamics Simulations

Residue protonation state was attributed according to the respective *pKa* values; Lys and Arg residues were modelled in protonated charged state (+1), aspartate and glutamate residues in deprotonated state with a point charge of (-1), Zn-coordinating cysteines in deprotonated state (CYM) and non-coordinating histidines (astacin) in uncharged monoprotonated state at the Nε^2 atom. Molecules were placed in a cubic box with edges at least 12 Å from the solute and solvated with the explicit TIP3P water model [3] (~15900 molecules for astacin, ~5500 for Sp1f2 and RD01, ~4900 for HP35 and RD02). Chloride or sodium counter-ions were added first to neutralize the total charge of the system and then added in equal proportion to achieve a 50 mM NaCl concentration. Energy minimization was done in two steps to remove eventual atom clashes in crystallographic, NMR structures or Rosetta outputted files: steepest descent minimization algorithm followed by a conjugated gradient algorithm (< 100 kJ/mol/nm). Short equilibration in a NPT ensemble was done next (Nosé-Hoover thermostat at 300 K with time-constant of 1.6 ps [4,5]; isotropic Parrinello-Rahman barostat at 1 bar with time-constant 5 ps [6,7]) with positional restrains for all hydrogen bonds in 3 consecutive steps of 100 ps each with the LINCS algorithm (order parameter 8, iteration level 2) and a force constant of 1000, 100 and 10 kJ/mol, respectively. Integration step was 2 fs and coordinates were saved each 25

ps, with long-range electrostatics being treated with the Particle-Mesh Ewald algorithm [8]. The “gromos” clustering method described by Piana *et al.* was employed to the concatenated trajectories, with a minimum of 10 structures per cluster and a cut-off of 3 Å between backbone atoms.[9] The 2D RMSD matrix of 40001x40001 (peptides) or 14000x14000 (astacin) elements was calculated, corresponding to equally spaced 50 ps frames. Each cluster was represented by the centroid structure, *i.e.* the one with smallest average distance to the remaining neighbours. Analysis of designed active site (d_{AB}, θ_B) done at each 50 ps frames. Production of all images was done using VMD 1.9.2 [10] and rendering of image files done with Tachyon.[11]

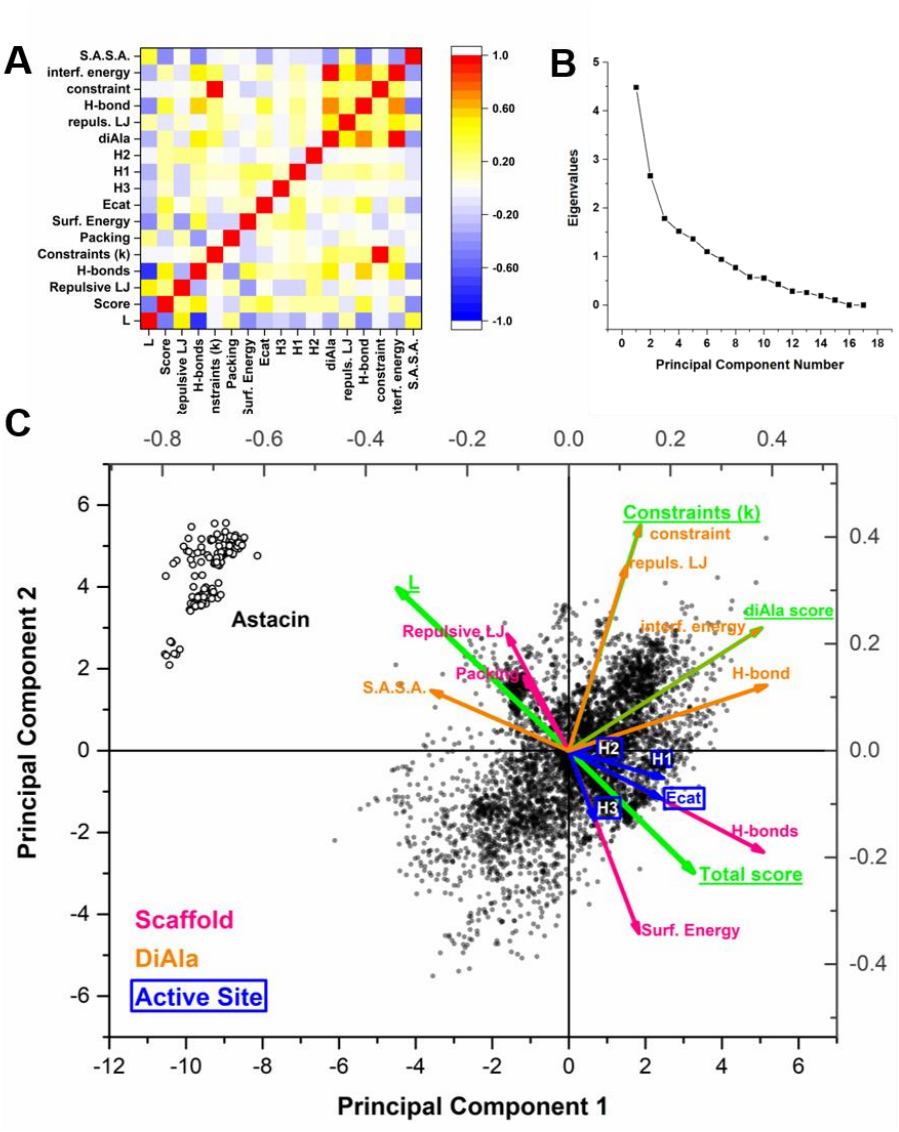

Figure S1 - Results from PCA of screened scaffolds.
Corresponding description of each one of the parameters given in 1). Selected parameters used for ranking of designs in green. Astacin designs in open circles, remaining scaffolds in closed circles

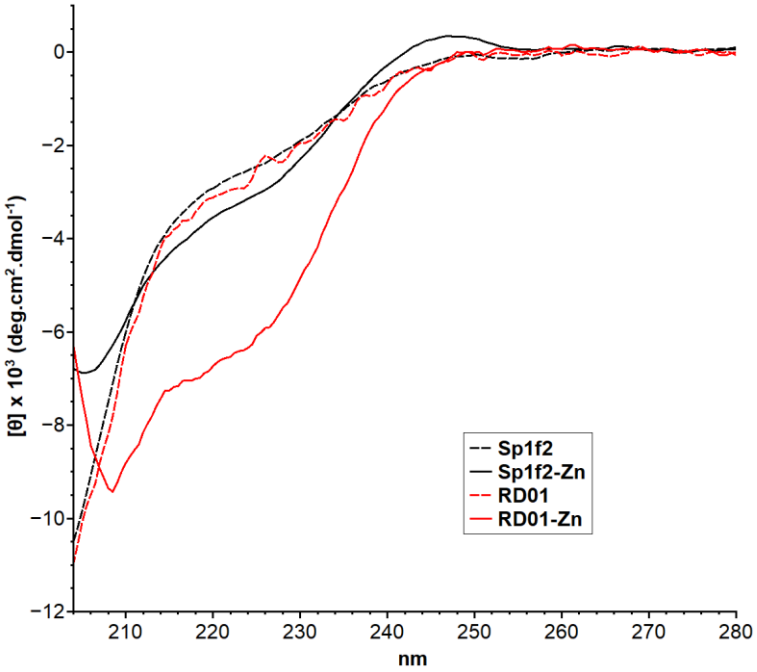

Figure S2 - – Comparison of CD spectra between native Sp1f2 and RD01.
Far-UV CD spectra of 25 µM free peptide (dashed lines) and zinc complex forms (solid lines) in 10 mM TRIS 50 mM NaCl at 25 °C, pH 8.0. Additions of $ZnCl_2$ were 37.5 µM for Sp1f2 an 100 µM for RD01. Spectra correspond to two replicates.

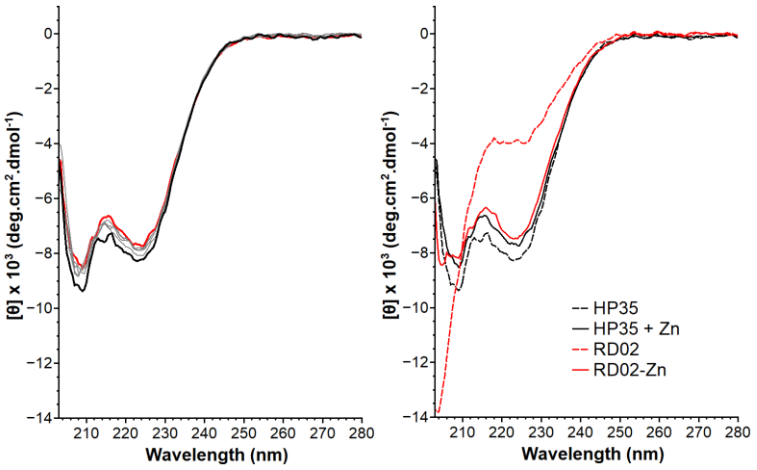

Figure S3 - Comparison of CD spectra between native HP35 and RD02.
Left: Far-UV CD spectra of 25 µM HP35 (black line) and upon addition of 150 µM $ZnCl_2$ (red line) in 10 mM HEPES 50 mM NaCl at 25 °C, pH 7.5. Right: Corresponding spectra of free peptide (dashed lines) and zinc complex forms (solid lines) of HP35 and RD02, 25 µM peptide and 150 µM $ZnCl_2$. Spectra correspond to two replicates.

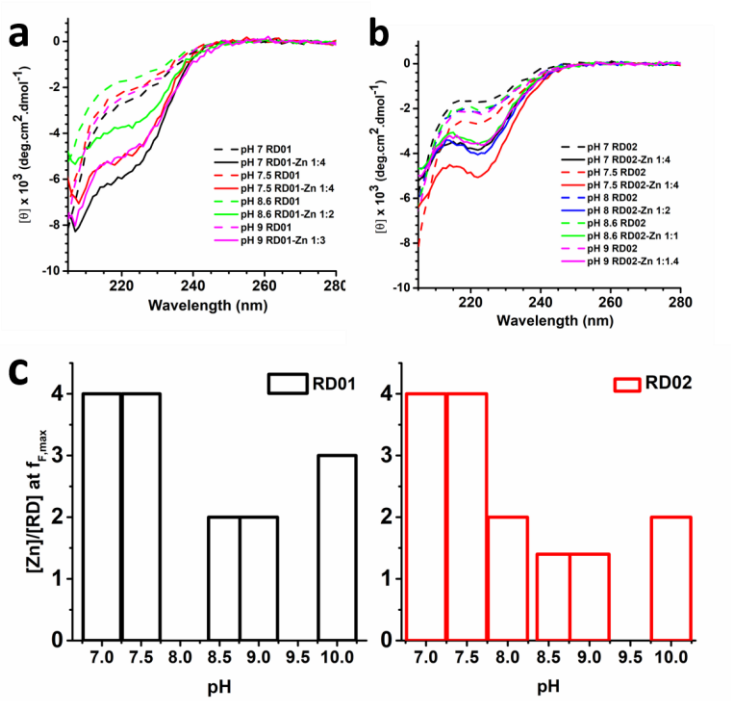

Figure S4 - CD spectra of RD01 and RD02 in free peptide and zinc complex forms for different pH values.

Free peptide and zinc-complex forms of (a) RD01 and (b) RD02, 25 µM concentration of peptide and corresponding peptide-Zn ratios at 25 °C. (c) Corresponding ratios at which the maximum ellipticity values for the zinc-complex forms were obtained.

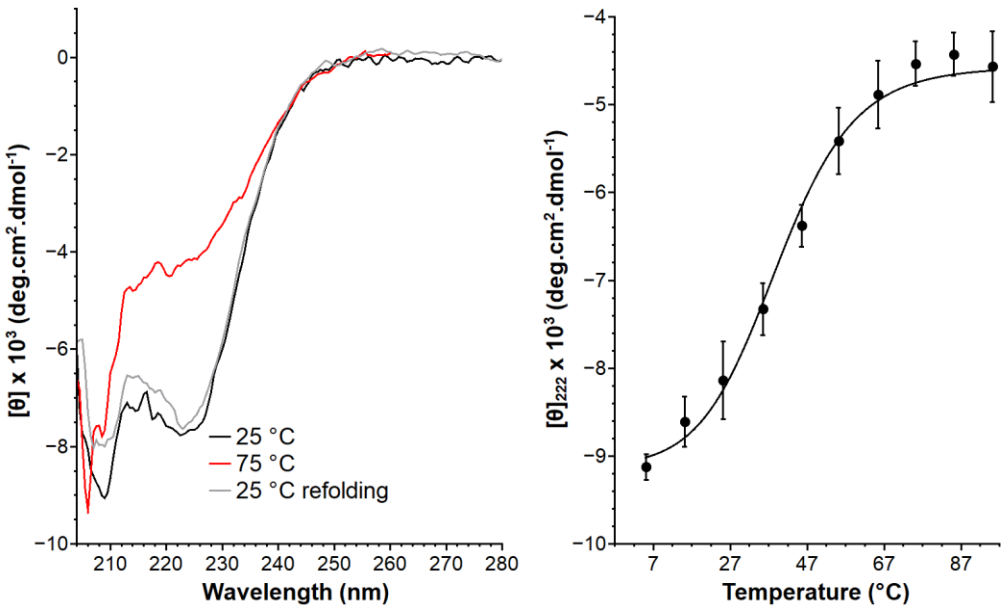

Figure S5 - Thermal unfolding of native HP35.

Left: Far-UV CD spectra of 25 µM HP35 in 10 mM HEPES 50 mM NaCl, pH 7.5 at 25 °C, 75 °C and after refolding at 25 °C. Right: Corresponding $[\theta]_{222}$ values as a function of temperature, solid lines correspond to the fit to the two-state transition model. Data corresponds to two replicates.

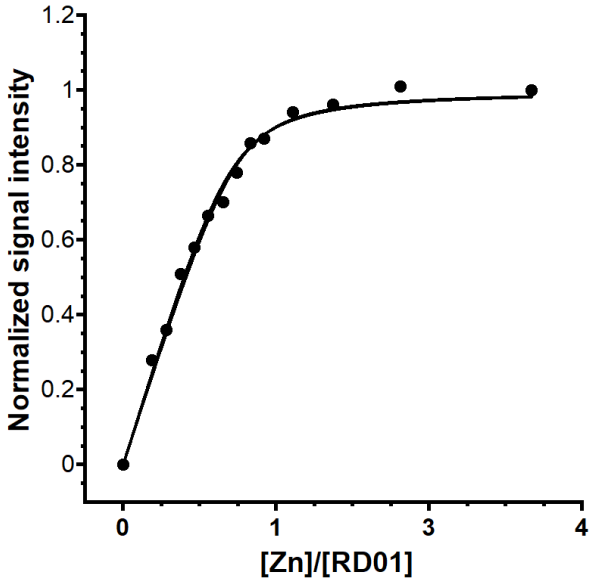

Figure S6 – ^{1}H NMR of RD01 signal at 1.05 ppm.

Data was obtained for 150 µM peptide in 50 mM NaCl, pH 7.5 with addition of 0-534 µM of $ZnCl_2$ at 25 °C.

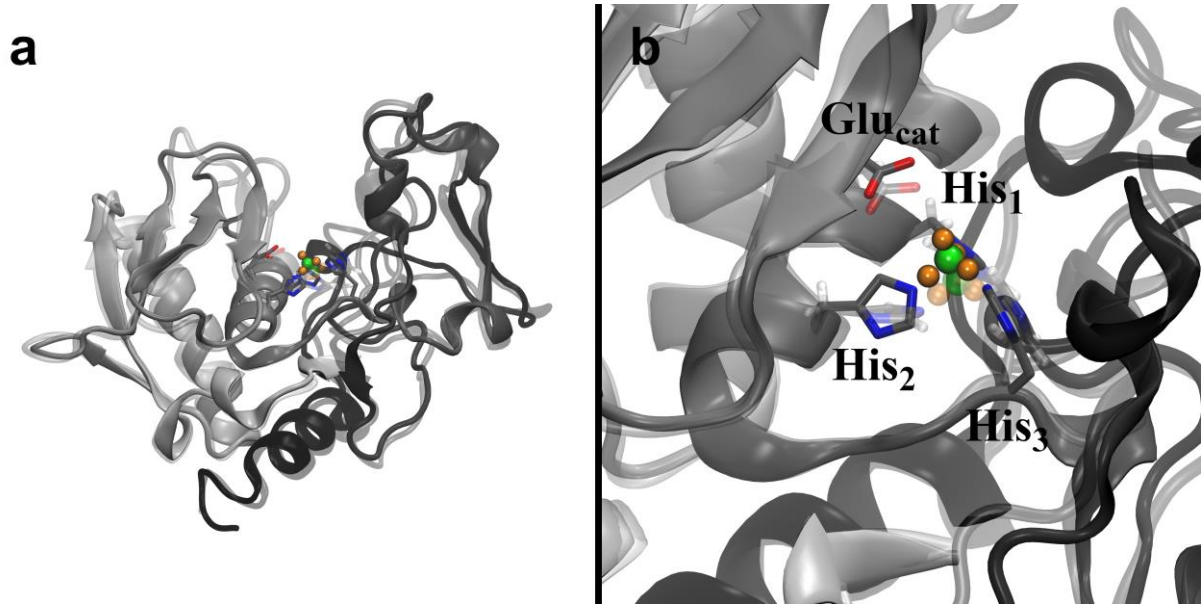

Figure S 7 - Cluster analysis of astacin MD simulations, (a) full structure and (b) detail of active site. Backbone in cartoon representation and colored based on residue index. Residues involved in metal interactions, atoms from the CaDA model shown in spheres, green for zinc ion and orange for dummy atoms. Cluster centroid and initial conformation in transparent and solid representations, respectively.

Table S1 - Geometrical parameters of AS from selected MA(M) structures. Subclan families and PDB identifiers on top.

Interaction		M10						M12				
		1I76	1MMP	1CIZ	1CAQ	1B8Y	1HFS	1QJI	4AIG	1ATL	3G42	$\bar{x} \pm \frac{\sigma}{\sqrt{n}}$
d_{AB}	His_1	2	2.1	2.2	2.2	2.2	1.9	2.2	2.1	2	2	2.1±0.1
	His_2	2	2.2	2.2	2.2	2.2	1.9	2.1	2.2	2.1	2	2.1±0.1
	His_3	2	2.1	2.2	2.2	2.2	1.8	1.9	2.3	2	2	2.1±0.2
	Glu_{cat}	5.1	4.9	5	5	5.2	5.5	4.7	5.2	4.6	5.1	5.0±0.3
θ_A	His_1	100.5	91.8	93.6	91.8	94.2	93.3	105	96	112.4	89.6	96.8±7.1
	His_2	88.4	94.9	88.4	96.6	93.3	88.2	108.8	83.9	106.5	92.6	94.2±8.1
	His_3	142.2	150.6	151.4	147.2	144.2	154.4	130.6	144.7	131.9	143	144.0±7.8
	Glu_{cat}	33	31	30.4	36.1	36.5	19.8	48.2	31.5	51.1	33.4	35.1±9.0
θ_B	His_1	126.7	126.1	129.4	128.2	132.5	129.3	133.1	128.8	131.3	118.9	128.4±4.1
	His_2	123.9	126.1	121.2	121.5	114.9	131.5	126.8	121	126.5	124.9	123.8±4.5
	His_3	126.6	117.3	119.1	122.6	121.6	124.7	126.2	131.4	122.9	130.5	124.3±4.5
	Glu_{cat}	88.5	96.1	93.1	94.7	90.8	83.3	85.3	94	98.8	93.3	91.8±4.8
χ_A	His_1	248.4	261.1	247.7	240.4	237.4	249	243.3	246.2	281.4	252.7	250.8±12.6
	His_2	143.9	158.3	142.1	134.4	131.9	145.7	134.2	143.5	172.3	153.2	146.0±12.4
	His_3	36.2	34.2	37.4	17.5	1.7	37	10.7	37.7	53.6	38.3	30.4±15.5
	Glu_{cat}	184.7	188.5	173.8	160.6	156.3	187.2	166.1	186	220	190.3	181.4±18.4
χ_{AB}	His_1	165.5	149.8	167.8	169.1	170.4	156.5	148.9	167.3	129.1	157.6	158.2±12.9
	His_2	208.6	197.9	191.3	198	198.3	198.3	197.4	201.9	198.9	191.2	198.2±4.9
	His_3	4.6	22.9	2.8	16.2	29.6	8.7	39.2	4.3	21.1	19.8	16.9±12.0
	Glu_{cat}	79.6	74.9	67.2	67.3	70.1	95.6	72.4	82	79.1	66.1	75.4±9.1
χ_B	His_1	168	174.8	160.6	155.6	154.7	176.9	164.6	161.9	182.3	171.2	167.1±9.2
	His_2	186	190.5	190.2	184.4	185.2	186.9	195	193	198.3	194.9	190.4±4.8
	His_3	162.6	163.4	173	176.8	163.9	167.5	164.9	171.3	165.1	158.1	166.7±5.6
	Glu_{cat}	138.7	145.7	140.3	141.3	143.8	148.4	151.6	148	151.5	141.2	145.1±4.7

Table S2 - Geometrical parameters of diAla substrate.

 # 1QJI_diala_conf.params

```
NAME dA1
IO_STRING dA1 Z
TYPE LIGAND
AA UNK
ATOM ZN1  Zn2p  X   1.96
ATOM  O2  OH    X   -0.70
ATOM  C1  CH1   X   -0.13
ATOM  O3  OOC   X   -0.80
ATOM  N3  Ntrp  X   -0.65
ATOM  C8  CH1   X   -0.13
ATOM  C2  CH3   X   -0.31
ATOM  H12 Hapo  X   0.06
ATOM  H13 Hapo  X   0.06
ATOM  H14 Hapo  X   0.06
ATOM  C5  COO   X   0.58
ATOM  N2  NH2O  X   -0.51
ATOM  H2  Hpol  X   0.39
ATOM  H3  Hpol  X   0.39
```

```
ATOM  O4  ONH2  X   -0.59
ATOM  H1  Hapo  X   0.06
ATOM  H7  Hpol  X   0.39
ATOM  C6  CH1   X   -0.13
ATOM  N1  Ntrp  X   -0.65
ATOM  C4  COO   X   0.58
ATOM  O1  ONH2  X   -0.59
ATOM  C3  CH3   X   -0.31
ATOM  H8  Hapo  X   0.06
ATOM  H10 Hapo  X   0.06
ATOM  H11 Hapo  X   0.06
ATOM  H16 Hpol  X   0.39
ATOM  C7  CH3   X   -0.31
ATOM  H4  Hapo  X   0.06
ATOM  H5  Hapo  X   0.06
ATOM  H6  Hapo  X   0.06
ATOM  H9  Hapo  X   0.06
ATOM  H15 Hpol  X   0.39
BOND  C1   O2
BOND  C1   O3
BOND  C1   N3
BOND  C1   C6
BOND  C2   C8
BOND  C2   H12
BOND  C2   H13
BOND  C2   H14
BOND  N1   C4
BOND  N1   C6
BOND  N1   H16
BOND  O1   C4
BOND  N2   C5
BOND  N2   H2
BOND  N2   H3
BOND  O2   H15
BOND  O2  ZN1
BOND  O4   C5
BOND  C3   C4
BOND  C3   H8
BOND  C3   H10
BOND  C3   H11
BOND  N3   C8
BOND  N3   H7
BOND  C5   C8
BOND  C6   C7
BOND  C6   H9
BOND  C7   H4
BOND  C7   H5
BOND  C7   H6
BOND  C8   H1
CHI 1 ZN1   O2   C1   O3
CHI 2  O2   C1   N3   C8
CHI 3  O2   C1   C6   N1
CHI 4  C6   N1   C4   O1
CHI 5  C1   C6   N1   C4
CHI 6  C1   N3   C8   C2
CHI 7  N3   C8   C5   N2
NBR_ATOM  O2
NBR_RADIUS 8.363764
ICOOR_INTERNAL   ZN1     0.000000    0.000000    0.000000  ZN1    O2    C1
ICOOR_INTERNAL    O2     0.000000  180.000000    1.849189  ZN1    O2    C1
ICOOR_INTERNAL    C1     0.000001   56.729696    1.595460   O2   ZN1    C1
ICOOR_INTERNAL    O3     5.414501   78.336182    1.568874   C1    O2   ZN1
ICOOR_INTERNAL    N3   119.370020   65.773055    1.655588   C1    O2    O3
ICOOR_INTERNAL    C8   -76.489396   61.101004    1.535813   N3    C1    O2
ICOOR_INTERNAL    C2    77.096851   69.172846    1.539788   C8    N3    C1
ICOOR_INTERNAL    H12 -116.166899   70.478464    1.089474   C2    C8    N3
ICOOR_INTERNAL    H13 -120.051541   70.526968    1.090604   C2    C8    H12
ICOOR_INTERNAL    H14 -119.923854   70.546616    1.090087   C2    C8    H13
```

```
ICOOR_INTERNAL    C5   121.054923   70.835105    1.524968   C8    N3    C2
ICOOR_INTERNAL    N2   132.297922   63.393354    1.341865   C5    C8    N3
ICOOR_INTERNAL    H2    -3.246935   59.118818    1.009561   N2    C5    C8
ICOOR_INTERNAL    H3  -179.985254   60.445997    1.009692   N2    C5    H2
ICOOR_INTERNAL    O4   179.726837   58.151996    1.223927   C5    C8    N2
ICOOR_INTERNAL    H1   119.995376   71.118126    1.089578   C8    N3    C5
ICOOR_INTERNAL    H7  -121.397122   72.908834    1.009422   N3    C1    C8
ICOOR_INTERNAL    C6   126.918397   69.610456    1.707063   C1    O2    N3
ICOOR_INTERNAL    N1    53.919212   64.020083    1.446771   C6    C1    O2
ICOOR_INTERNAL    C4  -101.124052   59.540397    1.324118   N1    C6    C1
ICOOR_INTERNAL    O1    -0.031823   56.993050    1.232007   C4    N1    C6
ICOOR_INTERNAL    C3  -178.207807   63.265011    1.513557   C4    N1    O1
ICOOR_INTERNAL    H8   -97.218306   69.813070    1.090471   C3    C4    N1
ICOOR_INTERNAL    H10  119.199821   68.909778    1.089870   C3    C4    H8
ICOOR_INTERNAL    H11  120.098134   72.723062    1.089461   C3    C4    H10
ICOOR_INTERNAL    H16 -179.110947   63.140534    0.980142   N1    C6    C4
ICOOR_INTERNAL    C7   127.125575   66.295147    1.525871   C6    C1    N1
ICOOR_INTERNAL    H4  -108.636956   70.497439    1.090028   C7    C6    C1
ICOOR_INTERNAL    H5  -120.078698   70.505253    1.090535   C7    C6    H4
ICOOR_INTERNAL    H6  -119.955610   70.572417    1.090338   C7    C6    H5
ICOOR_INTERNAL    H9   117.493922   78.793685    1.089756   C6    C1    C7
ICOOR_INTERNAL    H15  125.262060   73.810349    0.956392   O2   ZN1    C1
PDB_ROTAMERS 1QJI_diAla_conf_Zn_con.pdb
```

Table S3 – MA(M):diAla *cst* file (top) and *matcher* and *enzyme design* options (bottom).

```
# MAM:diAla cst file
# O2 corresponds to Ow atom. C1 to the tetrahedral carbon bound to Ow and Op.
# diAla has 3-letter code dA1.
# 6th column of distanceAB value set to 0 for non-bonded interaction, set to 1
for pseudocovalent interaction.
# When secondary algorithm is used, angle_A angle_B torsion_A torsion_AB
torsion_B commented out.
#Glu_cat - catalytic interaction
CST::BEGIN
  TEMPLATE::   ATOM_MAP: 1 atom_name: ZN1 O2 C1
  TEMPLATE::   ATOM_MAP: 1 residue3: dA1
  TEMPLATE::   ATOM_MAP: 2 atom_type: OOC ,    #either OE1 or OE2
  TEMPLATE::   ATOM_MAP: 2 residue1:  E
  CONSTRAINT:: distanceAB:   5.0  0.3  100  0    1  #2
  CONSTRAINT::    angle_A:  35.1  9.0   30  360  1  #2
  CONSTRAINT::    angle_B:  91.8  4.8   30  360  1  #1
  CONSTRAINT::  torsion_A: 181.4 18.4   30  360  1  #4
  CONSTRAINT:: torsion_AB:  75.4  9.1   30  360  1  #2
  CONSTRAINT::  torsion_B: 145.1  4.7   30  360  1  #1
CST::END
# His3 - Zn(II) 1st coord. sphere
CST::BEGIN
  TEMPLATE::   ATOM_MAP: 1 atom_name: ZN1 O2 C1
  TEMPLATE::   ATOM_MAP: 1 residue3: dA1
  TEMPLATE::   ATOM_MAP: 2 atom_type: Ntrp ,  #either ND1 or NE2
  TEMPLATE::   ATOM_MAP: 2 residue1:  H
  CONSTRAINT:: distanceAB:   2.1  0.2  100  1     1  #2
  CONSTRAINT::    angle_A: 144.0  7.8   30  360   1  #2
  CONSTRAINT::    angle_B: 124.3  4.5   30  360   1  #1
  CONSTRAINT::  torsion_A:  30.4 15.5   30  360   1  #3
  CONSTRAINT:: torsion_AB:  16.9 12.0   30  11.25 0  #1
  CONSTRAINT::  torsion_B: 166.7  5.6   30  360   1  #2
#ALGORITHM_INFO:: match      ;not commented out when secondary algorithm is used
#SECONDARY_MATCH: DOWNSTREAM ;not commented out when secondary algorithm is used
#ALGORITHM_INFO::END         ;not commented out when secondary algorithm is used
CST::END
# His1 - Zn(II) 1st coord. sphere
CST::BEGIN
  TEMPLATE::   ATOM_MAP: 1 atom_name:  ZN1 O2 C1
  TEMPLATE::   ATOM_MAP: 1 residue3: dA1
  TEMPLATE::   ATOM_MAP: 2 atom_type: Ntrp,   #either ND1 or NE2
```

```
  TEMPLATE::   ATOM_MAP: 2 residue1:  H
  CONSTRAINT:: distanceAB:   2.1  0.1 100  1     1  #1
  CONSTRAINT::    angle_A:  96.8  7.1  30  360   1  #2
  CONSTRAINT::    angle_B: 128.4  4.1  30  360   1  #1
  CONSTRAINT::  torsion_A: 250.8 12.6  30  360   1  #3
  CONSTRAINT:: torsion_AB: 158.2 12.9  30  11.25 0  #1
  CONSTRAINT::  torsion_B: 167.1  9.2  30  360   1  #2
#ALGORITHM_INFO:: match      ;not commented out when secondary algorithm is used
#SECONDARY_MATCH: DOWNSTREAM ;not commented out when secondary algorithm is used
#ALGORITHM_INFO::END         ;not commented out when secondary algorithm is used
CST::END
# His2 - Zn(II) 1st coord. sphere
CST::BEGIN
  TEMPLATE::   ATOM_MAP: 1 atom_name:  ZN1 O2 C1
  TEMPLATE::   ATOM_MAP: 1 residue3: dA1
  TEMPLATE::   ATOM_MAP: 2 atom_type: Ntrp  ,  #either ND1 or NE2
  TEMPLATE::   ATOM_MAP: 2 residue1:  H
  CONSTRAINT:: distanceAB:   2.1  0.1 100  1     1  #1
  CONSTRAINT::    angle_A:  94.2  8.1  30  360   1  #2
  CONSTRAINT::    angle_B: 123.8  4.5  30  360   1  #1
  CONSTRAINT::  torsion_A: 146.0 12.4  30  360   1  #3
  CONSTRAINT:: torsion_AB: 198.2  4.9  30  11.25 0  #1
  CONSTRAINT::  torsion_B: 190.4  4.8  30  360   1  #1
#ALGORITHM_INFO:: match       ;not commented out when secondary algorithm is used
#SECONDARY_MATCH: DOWNSTREAM  ;not commented out when secondary algorithm is used
#ALGORITHM_INFO::END          ;not commented out when secondary algorithm is used
CST::END
```

 # options_matcher.flags

```
-packing
 -ex1:level 3 #Chi'1 sampling level
 -ex2:level 3 #Chi'2 sampling level
 -ex2aro
 -ex1aro
 -use_input_sc
 -linmem_ig 10
-match
-bump_tolerance 0.2
 -filter_colliding_upstream_residues
 -
filter_upstream_downstream_collisions
 -output_format CloudPDB
 -enumerate_ligand_rotamers
 -dun10
-mute protocols.idealize
```

 # options_enzdes.flags

```
-dun10
-packing
 -use_input_sc
 -ex1:level 6 #Chi'1 sampling level
 -ex2:level 6 #Chi'2 sampling level
 -ex1aro:level 6
 -ex2aro:level 6
 -soft_rep_design
 -linmem_ig 10
-enzdes
-parser_read_cloud_pdb true
 -cst_opt
 -chi_min
 -bb_min
 -cst_design
 -cst_min
 -design_min_cycles 4
 -detect_design_interface
 -cut1 6.0
 -cut2 8.0
 -cut3 10.0
 -cut4 12.0
-score
   -weights enzdes.wts
-fix_catalytic_aa
-nstruct 1 #for design or -nstruct 10 for
full sequence design
```

Table S4 – Scaffolds screened with the MA(M):diAla model.

Scaffold	**Classification** (UniprotKB)	**Fold**	**Chain length (L)**	**PDB**	**#NMR X-ray**	**Secondary**	**Classical (UM)**
Trp-cage	De Novo Protein	α	20	1L2Y	38	- -	- -
VPg	Viral Protein P03300	α	22	2BBL	10	OK	E7H14H2H17
							E20H2H17H14
HIV gp120 C5 Domain	Viral Protein P19549	α	23	1MEQ	X-ray	OK	E9H22H5H3
Poneratoxin	Toxin P41736	α	25	1G92	10	OK	E21H6H15H17
							E23H14H16H19
FBP28 WW Domain	SH3 Domain Q8CGF7	β	27	1E0L	10	OK	E9H26H21H23
Fibritin C-terminal - Foldon	Viral Protein P10104	β	27	4NCU	X-ray	- -	- -
CCK2E3	Hormone/Growth Factor Receptor P32239	α	30	1L4T	1	OK	- -
pGolemi	De Novo Protein	α	30	2K76	10	OK	E13H6H7H16
							E26H6H23H2
Parathyroid Hormone	Hormone/Growth Factor P01270	α	31	1FVY	20	OK	- -
Cholecystokinin A	Hormone/Growth Factor P32238	α	31	1HZN	X-ray	- -	- -
DNA polymerase iota	Ubiquitin binding domain Q9UNA4	α	32	2L0G	20	OK	E685H700H679H696
							E688H680H699H679
							E688H680H703H679
							E688H681H699H683
							E688H703H679H682
							E691H680H679H683
							E700H680H699H703
							E702H682H680H699
							E706H680H703H699
							E706H682H680H699
							E706H682H703H699
P-element Somatic Inhibitor	Nuclear Protein Q7JPS0	α	33	2BN6	29	OK	- -
Human Villin Headpiece	Actin Binding P09327	α	34	1UNC	25	OK	E14H29H6H25
							E14H29H17H25
							E18H26H25H22
							E26H6H25H29
							E26H17H25H29
							E28H6H10H17
							E29H14H17H6
Advillin Human	Actin Binding O75366	α	36	1UND	25	- -	- -
pPYY	Hormone/Growth Factor P68005	α	36	1RU5	20	OK	E3H24H5H20
							E7H24H5H20
							E19H11H6H16
							E27H36H34H24
							E30H6H27H23
							E36H20H24H5
WW Domain Prototype	De Novo Protein	β	37	1E0M	10	OK	E5H27H22H33
							E5H27H25H33
							E5H27H24H8
							E5H27H24H22
							E27H5H8H24
E3-binding domain	Glycolysis P0AFG6	α	37	1BBL	1	OK	E17H39H16H20
Alpha-T-alpha	De Novo Protein	α	38	1ABZ	23	OK	E1H32H36H4
							E1H33H36H4
							E18H28H24H15

							E28H21H25H15
							E31H14H11H24
							E31H14H11H21
							E31H21H11H28
							E31H21H28H24
							E31H21H11H24
							E31H14H11H28
							E33H3H32H36
							E33H4H32H36
							E35H11H7H31
							E35H11H32H28
CRE-BP1	DNA binding regulatory protein P15336	α+β	38	1BHI	20	OK	E5H15H8H10
							E19H6H17H4
							E28H11H9H31
Phage Scaffolding Protein	Viral Protein P26748	α	40	2GP8	1	OK	E13H28H16H32
MafG	DNA binding protein O54790	α	41	1K1V	20	OK	E38H53H37H41
							E38H53H37H49
							E41H34H38H53
Phosphoprotein XD domain	Viral protein P03422	α	44	2K9D	20	OK	E468H504H501H473
							E468H504H501H474
							E468H504H501H505
							E468H505H474H501
							E500H473H504H501
							E502H463H498H467
							E504H468H501H497
GA module	Albumin Binding Protein Q51911	α	45	1PRB	1	OK	- -
HHR23A	C-terminal UBA domain P54725	α	45	1IFY	10	OK	E164H171H177H168
FAF UBA domain	Apoptosis Q9UNN5	α	45	3E21	X-ray	- -	- -
HIV Vpu	HIV protein P19554	α	45	1VPU	X-ray	- -	- -
UBA Domain	Ligase Q13191	α	46	2JNH	15	OK	E8H25H7H11
							E8H21H25H15
							E8H21H11H15
							E29H5H7H33
Sda antikinase	Signaling Protein Q7WY62	α	46	1PV0	25	- -	- -
ATP synthase ipsilon chain	Hydrolase Q5KUJ4	α	46	2E5T	20	OK	E101H124H97H120
							E104H97H101H120
							E104H124H97H120
							E104H124H101H120
							H119H99H100H116
							E127H101H124H97
							E127H101H120H97
dihydrolipoyllysine acetyl transferase	Transferase P11961	α	47	1W4E	20	OK	- -
Swa2p	Protein Binding Q06677	α	47	1PGY	20	OK	E4H29H7H25
							E19H47H27H37
							E19H47H27H41
							E26H47H30H27
							E27H41H37H19
							E27H17H37H19
							E27H17H19H41
							E27H45H41H19
							E33H7H29H10
							E44H27H41H31
							E44H27H41H37

							E46H37H27H41
LysM Domain	Hydrolase P0AEZ7	α+β	48	1E0G	20	OK	E7H28H34H24
							E7H28H24H13
							E48H30H26H46
Lambda-Integrase	Viral Protein P03700	α+β	48	1KJK	25	OK	E15H52H55H14
							E27H19H17H34
							E29H52H55H14
							E31H35H33H28
							E31H58H28H30
							E49H14H13H52
							E51H31H30H28
							E51H31H28H35
							E51H33H28H35
							E54H33H30H28
Translation Initiatior factor 2 N-ter	Translation P0A705	α	49	1ND9	10	OK	- -
CSTF-64	Nuclear Protein P33240	α	49	2J8P	30	OK	E530H565H534H561
							E535H565H534H561
							E537H530H561H534
							E544H570H541H567
							E545H555H542H563
							E546H538H551H545
							E546H538H552H545
							E546H563H551H545
							E546H563H552H545
							E551H538H555H552
							E551H563H555H552
							E560H532H536H557
POB	Transferase Q8ZUR6	α	51	1W4J	20	OK	E167H138H164H142
NTL9	RNA Binding Protein P02417	α+β	51	2HBB	X-ray	OK	- -
Engrailed Homeodomain	DNA Binding Protein P02836	α	54	1ENH	X-ray	OK	E34H15H38H19
Protein G	Protein Binding P06654	α+β	56	2LGI	10	OK	- -
Protein A (Sp. aureus)	Protein Binding P38507	α	58	4NPE	X-ray	OK	- -
Thermolysin C-Ter	Hydrolase P00800	α	62	1TRL	8	OK	E300H265H262H295
							E302H265H262H295
							E309H284H288H267
Protein L	Immune System Q51912	α+β	64	2JZP	20	OK	E6H51H55H58
							E41H34H38H47
							E44H18H12H10
							E52H9H57H59

Table S5 – Buffer compositions and 4-nitrophenol extinction coefficients.

pH	**Buffer**		**NaCl**	ε_{400} ($M^{-1}cm^{-1}$)
7.0	HEPES	10 mM (binding) 40 mM (catalysis)	50 mM	8739±261
7.5				12754±201
8.0	TRIS/CHES			17674±455
8.6	CHES			26166±122
9.0				19302±155

Table S6 – Cluster analysis of MD simulations.

Scaffold	**RMSD matrix** [min, max] Å	**Number clusters** (cut-off 3 Å)	**# top clusters** (> 80% pop. Time)
Sp1f2	[0.3, 7.3]	5	1
RD01	[0.3, 14.0]	165	6
HP35	[0.3, 9.1]	29	1
RD02	[0.4, 12.2]	165	7
Astacin	[0.5, 4.1]	1	1

References

1 F. Grams, V. Dive, A. Yiotakis, I. Yiallouros, S. Vassiliou, R. Zwilling, W. Bode and W. Stöcker, *Nat. Struct. Mol. Biol.*, 1996, **3**, 671–675.

2 N. M. O'Boyle, M. Banck, C. A. James, C. Morley, T. Vandermeersch and G. R. Hutchison, *J. Cheminform.*, 2011, **3**, 33.

3 W. L. Jorgensen, J. Chandrasekhar, J. D. Madura, R. W. Impey and M. L. Klein, *J. Chem. Phys.*, 1983, **79**, 926.

4 S. Nosé, *Mol. Phys.*, 1984, **52**, 255–268.

5 W. G. Hoover, *Phys. Rev. A*, 1985, **31**, 1695–1697.

6 M. Parrinello and A. Rahman, *J. Appl. Phys.*, 1981, **52**, 7182–7190.

7 S. Nosé and M. L. Klein, *Mol. Phys.*, 1983, **50**, 1055–1076.

8 T. Darden, D. York and L. Pedersen, *J. Chem. Phys.*, 1993, **98**, 10089–10092.

9 X. Daura, K. Gademann, B. Jaun, D. Seebach, W. F. Van Gunsteren and A. E. Mark, *Angew. Chem. Int. Ed*, 1999, **38**, 38: 236-240.

10 W. Humphrey, a Dalke and K. Schulten, *J. Mol. Graph.*, 1996, **14**, 33–8, 27–8.

11 J. Stone, University of Missouri--Rolla, 1998.